

# **Nonlinear Optics (WiSe 2017/18)**

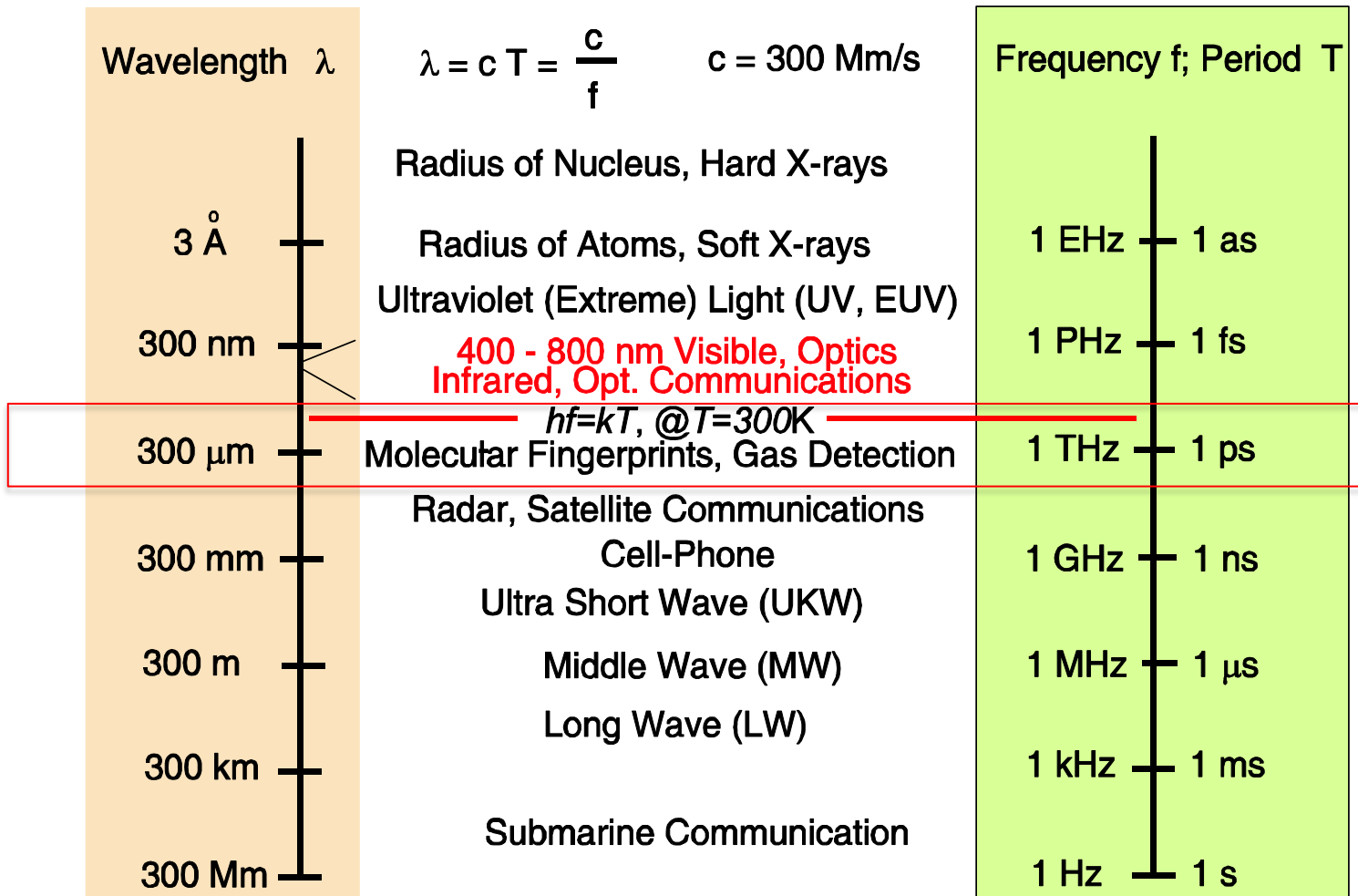
## **Lecture 21: January 11, 2018**

### **11 Terahertz generation and applications**

.....

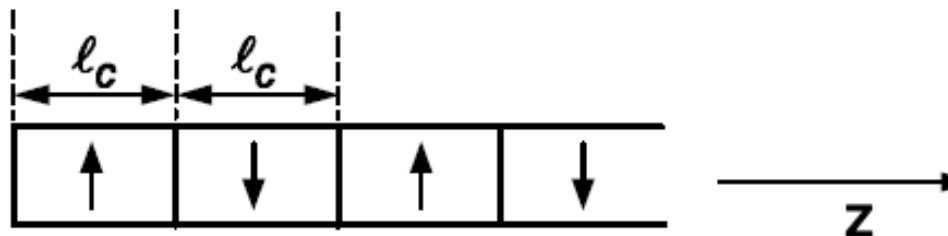
#### **11.2.2 Optical rectification by Quasi-Phase Matching (QPM)**

# 11 Terahertz generation and applications



0.3 – 30 THz

## 11.2.2 Optical rectification by Quasi-Phase Matching (QPM)



$$d_{eff}(z) = \sum_{m=-\infty}^{+\infty} d_m e^{jm\kappa z}$$

**Periodically poled crystal**

$$\begin{aligned} \Delta k &= \frac{\partial k_{opt}(\omega)}{\partial \omega} \Big|_{\omega_0} \Omega - k_{THz}(\Omega) + m \frac{2\pi}{\Lambda} = \left( \frac{1}{v_{g,opt}} - \frac{1}{v_{p,THz}} \right) \Omega + m \frac{2\pi}{\Lambda} \\ &= \left( \frac{n_{g,opt} - n_{p,THz}}{c} \right) \Omega + m \frac{2\pi}{\Lambda} = 0 \\ \rightarrow \quad \Lambda &= m \frac{\lambda_{THz}}{n_{p,THz} - n_{g,opt}}. \end{aligned}$$

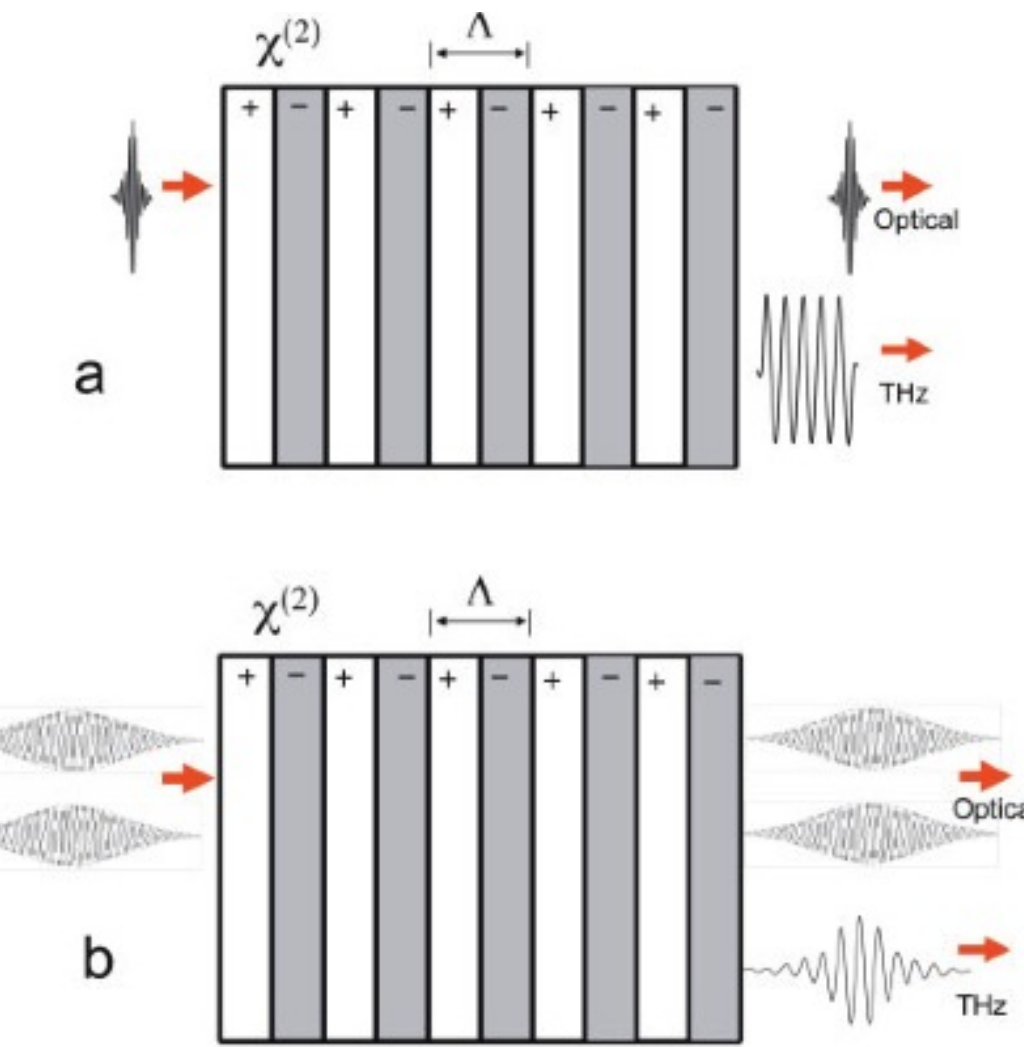


**Figure 11.10:** Schematic illustration of collinear THz-wave generation in a nonlin- ear crystal with periodically inverted sign of  $\chi(2)$ . (a) Optical rectification with femtosecond pulses, (b) difference-frequency generation with two picosecond pulses ( $\Omega = \omega_3 - \omega_2$ ) [10].

## Plane-wave analysis of optical-to-THz conversion in QPM crystals with ultrashort pulses

$$E_{opt}(t) = Re\{E_0 e^{-t^2/\tau^2} e^{j\omega_0 t}\} = \frac{1}{2}\{E_0 e^{-t^2/\tau^2} e^{j\omega_0 t} + c.c.\},$$

$$\hat{E}_{opt}(\omega) = \frac{E_o \tau}{2\sqrt{\pi}} \exp\left(-\frac{\tau^2 \omega^2}{4}\right)$$

$$\begin{aligned} \frac{d\hat{E}_{THz}(\Omega, z)}{dz} &= -j \frac{\Omega}{c n_{p, THz}} \frac{d_{eff}^{QPM}}{4\pi} \int_{-\infty}^{+\infty} \exp\left(-\frac{\tau^2 (\omega + \Omega)^2}{4}\right) \exp\left(-\frac{\tau^2 \omega^2}{4}\right) d\omega \\ &= -j \frac{\Omega}{c n_{p, THz}} \frac{d_{eff}^{QPM}}{2\sqrt{2\pi}} \exp\left(-\frac{\tau^2 \Omega^2}{8}\right) e^{j\Delta k(\Omega)z}. \end{aligned} \quad (11.23)$$

$$\left|\hat{E}_{THz}(\Omega, z)\right|^2 = \frac{\Omega^2}{c^2 n_{p, THz}^2} \frac{d_{eff}^{QPM,2}}{8\pi} \exp\left(-\frac{\tau^2 \Omega^2}{4}\right) L^2 \text{sinc}^2\left(\frac{\Delta k(\Omega)L}{2}\right) \quad (11.24)$$

$$\text{with } \Delta k(\Omega) = \Delta k = \frac{n_{g,opt} - n_{p, THz}}{c} + m \frac{2\pi}{\Lambda} \quad (11.25)$$

$$d_{eff}^{QPM} = \frac{2}{\pi} d_{eff}$$

# Optical to THz conversion efficiency

$$\eta_{THz}^{PW} = \frac{\text{Fluence THz}}{\text{Fluence (pump)}}$$

$$F_{pump} = \frac{c\varepsilon_0 n_{p,opt}}{2} \int_{-\infty}^{+\infty} |E_{opt}(t, 0)|^2 dt = \sqrt{\frac{\pi}{2}} \frac{c\varepsilon_0 n_{p,opt}}{2} E_o^2 \tau$$

and THz fluence

$$F_{THz} = \frac{c\varepsilon_0 n_{p,THz}}{2} \int_{-\infty}^{+\infty} |E_{THz}(t, L)|^2 dt = \frac{c\varepsilon_0 n_{p,THz}}{2} 2\pi \int_{-\infty}^{+\infty} |\hat{E}_{THz}(\Omega, z)|^2 d\Omega \quad (11.28)$$

where we used Parceval's theorem

$$\int_{-\infty}^{+\infty} |f(t)|^2 dt = 2\pi \int_{-\infty}^{+\infty} |\hat{f}(\Omega)|^2 d\Omega. \quad (11.29)$$

Thus, we obtain

$$N = \frac{L}{\Lambda}$$

$$\eta_{THz}^{PW} = \frac{\Omega^2 d_{eff}^{QPM,2} E_o^2 \tau}{2\sqrt{2\pi} c^2 n_{p,opt} n_{p,THz}} L^2 \int_0^{+\infty} \exp\left(-\frac{\tau^2 \Omega^2}{4}\right) \operatorname{sinc}^2\left(\frac{\pi}{2} \frac{\Omega - \Omega_0}{\Delta\Omega}\right) d\Omega,$$

$$\text{with } \Omega_0 = \frac{2\pi c}{\Lambda(n_{g,opt} - n_{p,THz})} \text{ and } \Delta\Omega = \frac{2\pi c}{L(n_{g,opt} - n_{p,THz})} = \frac{\Lambda}{L} \Omega_0 \quad (11.31)$$

$$\begin{aligned}
\eta_{THz}^{PW,sp} &= \frac{\Omega^2 d_{eff}^{QPM,2} E_o^2 c}{2\sqrt{2\pi}c^2 n_{p,opt} n_{p,THz}} L^2 g_1(\Omega_0) 2 \Delta\Omega = \\
&= \frac{\Omega^2 d_{eff}^{QPM,2} E_o^2 \tau}{c n_{p,opt} n_{p,THz}} \frac{\sqrt{2\pi}}{(n_{g,opt} - n_{p,THz})} L g(\Omega_0) \\
&= \frac{2\Omega^2 d_{eff}^{QPM,2} L}{\varepsilon_0 c^2 n_{p,opt}^2 n_{p,THz} (n_{g,opt} - n_{p,THz})} g_1(\Omega_0) F_{pump} \quad (11.32)
\end{aligned}$$

$$\text{with } g_1(\Omega_0) = \exp\left(-\frac{\tau^2 \Omega_0^2}{4}\right) = \exp\left(-(\pi f_{THz} \tau)^2\right) \text{ and} \quad (11.33)$$

$$2 \Delta\Omega = \int_{-\infty}^{+\infty} \operatorname{sinc}^2\left(\frac{\pi}{2} \frac{\Omega - \Omega_0}{\Delta\Omega}\right) d\Omega \quad (11.34)$$

## Influence of optical bandwidth

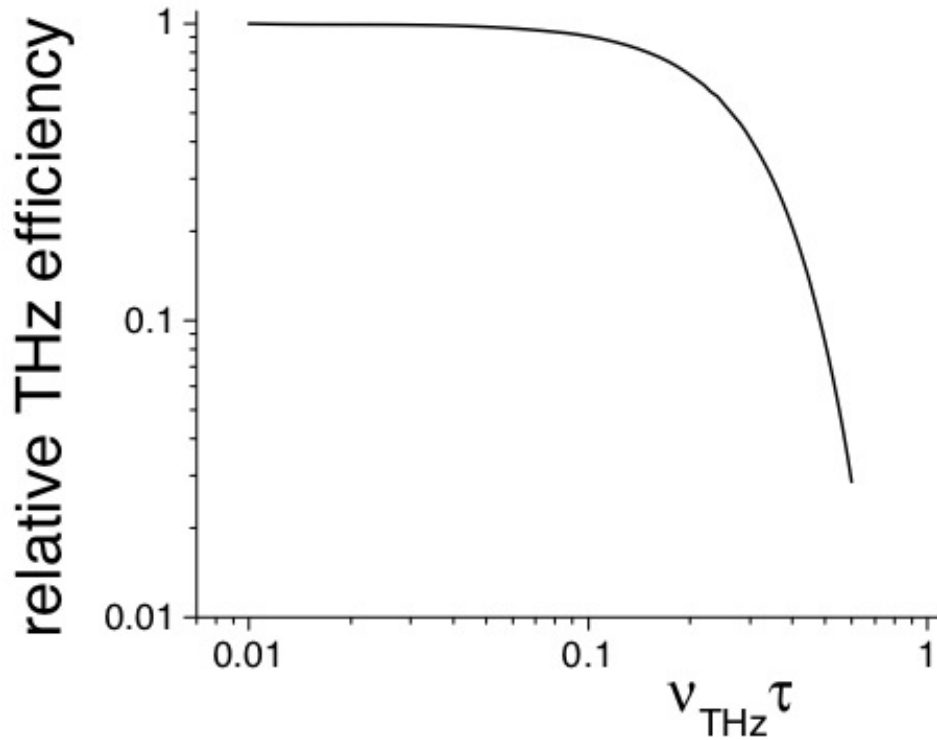


Figure 11.11: Relative THz generation reduction due to  $g_1(\Omega_0)$ .

## For long pulses

$$\begin{aligned}
 \eta_{THz}^{PW,lp} &= \frac{\Omega^2 d_{eff}^{QPM,2} E_o^2 \tau}{2\sqrt{2\pi}c^2 n_{p,opt} n_{p,THz}} L^2 \int_0^{+\infty} e^{\left(-\frac{\tau^2(\Omega-\Omega_0)^2}{4}\right)} \operatorname{sinc}^2\left(\frac{\pi}{2} \frac{\Omega - \Omega_0}{\Delta\Omega}\right) d\Omega \quad (11.35) \\
 &= \frac{\Omega^2 d_{eff}^{QPM,2} E_o^2 \tau}{2\sqrt{2\pi}c^2 n_{p,opt} n_{p,THz}} L^2 \int_0^{+\infty} e^{\left(-\frac{\tau^2(\Omega')^2}{4}\right)} \operatorname{sinc}^2\left(\frac{\pi}{2} \frac{\Omega'}{\Delta\Omega}\right) d\Omega'. \quad (11.36)
 \end{aligned}$$

**Walk-off**

$$l_w = \frac{\sqrt{\pi} c \tau}{(n_{g,opt} - n_{p,THz})}$$

$$\begin{aligned}
 \eta_{THz}^{PW,lp} &= \frac{\Omega^2 d_{eff}^{QPM,2} E_o^2}{2\sqrt{2\pi}c^2 n_{p,opt} n_{p,THz}} L^2 \int_0^{+\infty} \exp\left(-\frac{y^2}{4}\right) \operatorname{sinc}^2\left(\frac{\sqrt{\pi}}{2} \frac{L}{l_w} y\right) dy, \\
 \eta_{THz}^{PW,lp} &= \frac{\Omega^2 d_{eff}^{QPM,2} E_o^2}{\sqrt{2}c^2 n_{p,opt} n_{p,THz}} \frac{l_w L}{\pi} g_2\left(\frac{2l_w}{L}\right) \\
 g_2(x) &= \int_0^{+\infty} \exp\left(-\frac{x^2 \mu^2}{\pi}\right) \operatorname{sinc}^2(\mu) d\mu, \text{ with } x = \frac{2l_w}{L}.
 \end{aligned}$$

# Influence of walk-off

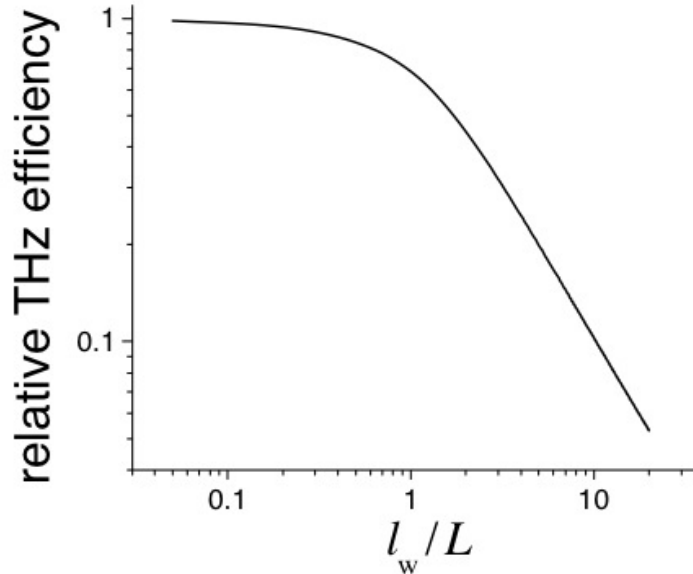


Figure 11.12: Relative THz generation reduction due to  $g_2(2\frac{l_w}{L})$ .

## Very long pulses

$$\begin{aligned}\eta_{THz}^{PW,lp \rightarrow \infty} &= \frac{\Omega^2 d_{eff}^{QPM,2} E_o^2}{2\sqrt{2\pi}c^2 n_{p,opt} n_{p,THz}} L^2 \\ &= \frac{\Omega^2 d_{eff}^{QPM,2}}{\pi \varepsilon_0 c^3 n_{p,opt}^2 n_{p,THz}} \frac{F_{pump}}{\tau} L^2,\end{aligned}$$

# Optimal length of the EO crystal

$$\eta_{THz}(L) \sim \frac{1}{\alpha_{THz}} [1 - e^{-\alpha_{THz} L}] = L_{eff}$$

$$\eta_{THz}(L) \sim g_3 L, \text{ with } g_3 = \frac{1}{\alpha_{THz} L} [1 - e^{-\alpha_{THz} L}]$$

For  $L = 1/\alpha_{THz}$ ,  $g_3 = 0.63$ .

## Optimal focusing

$$\eta_{THz} = \frac{U_{THz}}{U_{pump}} = g_1 g_3 \frac{2\Omega^2 d_{eff}^{QPM,2} L}{\varepsilon_0 c^2 n_{p,opt}^2 n_{p,THz} (n_{g,opt} - n_{p,THz})} \frac{U_{pump}}{\pi w^2}$$

$\xi = (\lambda L / 2\pi n_{THz} w^2)$ , where  $\lambda$  is the THz wavelength

**Ratio between crystal length and THz Rayleigh range**

# Enhancement factor

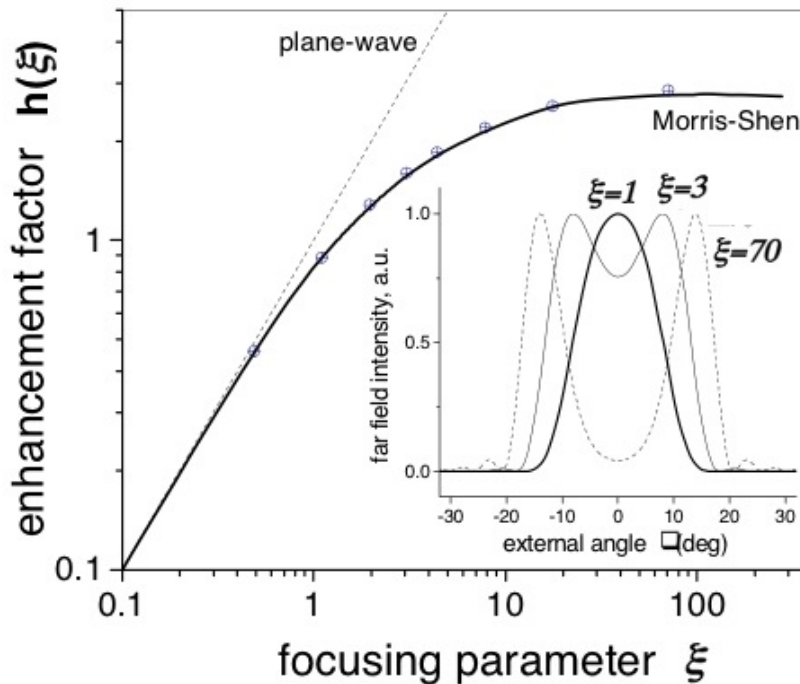


Figure 11.13: Enhancement factor  $h$  as a function of the focusing parameter  $\xi$ . Solid curve is based on Ref. [26]. Dashed curve – plane-wave approximation. Dots represent calculations based on the Green's function method. Inset: far-field THz intensity profiles at different  $\xi$  for a 1-cm-long GaAs.

## Cascading and red shift

optical pulse spectrum will be red-shifted by  $\Delta\omega/\omega_0 \sim \eta_{THz}$ :  
 $N = 0.5 \times (\text{acceptance bandwidth}) / (\text{terahertz frequency})$ .

$$\begin{aligned}\frac{d\Delta k}{d\omega} &= \frac{\Omega}{c} \frac{dn_{g,opt}(\omega)}{d\omega} = \frac{\Omega}{c} \frac{dn_{g,opt}(\lambda)}{d\lambda} \frac{d\lambda}{d\omega} \\ &= \frac{\Omega}{c} \frac{dn_{g,opt}(\lambda)}{d\lambda} \frac{\lambda^2}{2\pi c}\end{aligned}$$

$$\frac{d\Delta k}{d\omega} L \Delta\omega_{acc} = 2\pi$$

$$\Delta\omega_{acc} = \frac{2\pi c\omega}{L\Omega} \left( \lambda \frac{dn_{g,opt}(\lambda)}{d\lambda} \right)^{-1}.$$

## Cascading and red shift

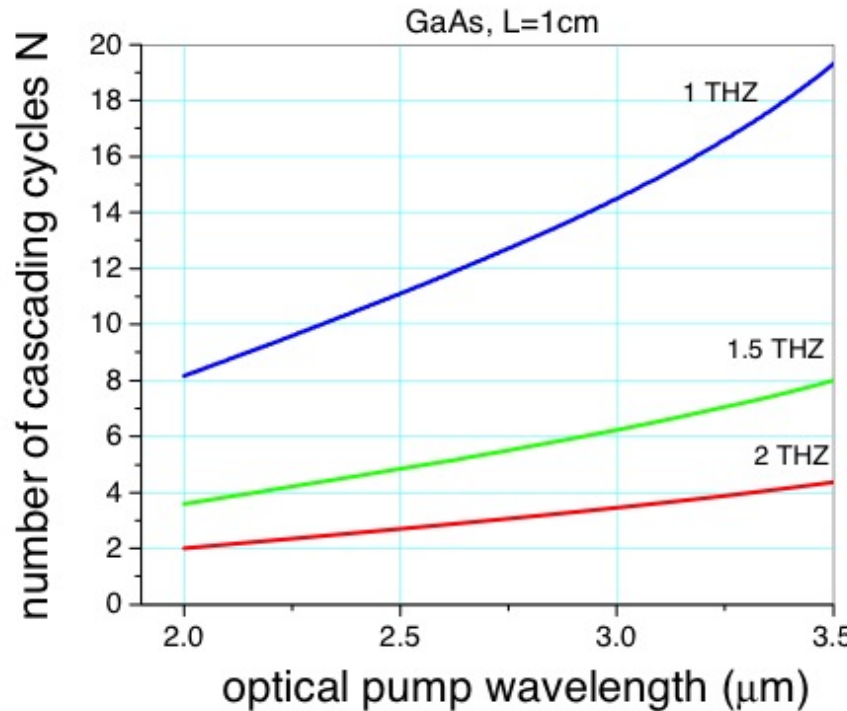


Figure 11.14: Number of THz cascading cycles as a function of THz frequency and pump wavelength for GaAs,  $L = 1\text{ cm}$ .

## Summary

$$FOM_1 = \frac{d_{eff}^2}{n_{p,opt}\alpha_{THz}} \quad (11.45)$$

or

$$FOM_2 = \frac{d_{eff}^2}{n_{p,opt}^2(n_{p,THz} - n_{g,opt})}. \quad (11.46)$$

If the maximum propagation distance is limited by the Kerr effect, the critical FOM becomes

$$FOM_3 = \frac{\lambda_{opt} d_{eff}^2}{n_{p,opt}^2 n_{p,THz} \alpha_{THz} n_2}. \quad (11.47)$$